

A PROPER MOTION STUDY OF THE HARO 6-10 OUTFLOW: EVIDENCE FOR A SUBARCSECOND BINARY

BRUCE A. WILKING

Department of Physics and Astronomy, University of Missouri-St. Louis and
1 University Boulevard, St. Louis, MO 63121

KEVIN B. MARVEL

American Astronomical Society and
2000 Florida Avenue, NW, Suite 400, Washington, DC 20009

MARK J. CLAUSSEN

National Radio Astronomy Observatory (NRAO) Array Operations Center
P.O. Box 0 and
1003 Lopezville Road, Socorro, NM 87801

BRADLEY M. GERLING

Department of Physics and Astronomy, University of Missouri-St. Louis and
1 University Boulevard, St. Louis, MO 63121

ALWYN WOOTTEN

NRAO and
520 Edgemont Road, Charlottesville, VA 22903-2475

AND

ERIKA GIBB

Department of Physics and Astronomy, University of Missouri-St. Louis and
1 University Boulevard, St. Louis, MO 63121

Draft version July 29, 2021

ABSTRACT

We present single-dish and VLBI observations of an outburst of water maser emission from the young binary system Haro 6-10. Haro 6-10 lies in the Taurus molecular cloud and contains a visible T Tauri star with an infrared companion 1.3'' north. Using the Very Long Baseline Array, we obtained five observations spanning 3 months and derived absolute positions for 20 distinct maser spots. Three of the masers can be traced over 3 or more epochs, enabling us to extract absolute proper motions and tangential velocities. We deduce that the masers represent one side of a bipolar outflow that lies nearly in the plane of the sky with an opening angle of $\sim 45^\circ$. They are located within 50 mas of the southern component of the binary, the visible T Tauri star Haro 6-10S. The mean position angle on the sky of the maser proper motions ($\sim 220^\circ$) suggests they are related to the previously observed giant Herbig-Haro (HH) flow which includes HH 410, HH 411, HH 412, and HH 184A-E. A previously observed HH jet and extended radio continuum emission (mean position angle of $\sim 190^\circ$) must also originate in the vicinity of Haro 6-10S and represent a second, distinct outflow in this region. We propose that a yet unobserved companion within 150 mas of Haro 6-10S is responsible for the giant HH/maser outflow while the visible star is associated with the HH jet. Despite the presence of H₂ emission in the spectrum of the northern component of the binary, Haro 6-10N, none of outflows/jets can be tied directly to this young stellar object.

Subject headings: ISM: jet and outflows - masers stars: T Tauri stars, Haro 6-10, GV Tau, IRAS 04263+2426

1. INTRODUCTION

Haro 6-10 (R.A.(2000) $4^h 29^m 23.7^s$, decl.(2000.0) $+24^\circ 33' 00''$) is a young binary system containing a visible T Tauri star (Haro 6-10S also known as GV Tau S)

and an infrared companion (Haro 6-10N also known as GV Tau N). They lie in the L 1534 molecular core in the Taurus cloud (140 pc, Elias 1978; Torres *et al.* 2009) and are separated by 1.3'' (180 AU) at a position angle of 355 degrees (Leinert & Haas 1989). Both components exhibit late-type photospheres (K7-M2) with luminosities and masses on the order of the Sun's (Goodrich 1986, Doppmann *et al.* 2008). Haro 6-10N, the more massive of the two objects, is apparently obscured by an edge-on disk and overtakes Haro 6-10S in brightness

Electronic address: bwilking@umsl.edu
Electronic address: marvel@aas.org
Electronic address: mcلاusse@nrao.edu
Electronic address: bmg5333@truman.edu
Electronic address: awootten@nrao.edu
Electronic address: gibbe@umsl.edu

at wavelengths $\geq 4.8 \mu\text{m}$ (Leinart & Haas 1989; Menard *et al.* 1993). Both components of the Haro 6-10 system are well-studied with high-resolution infrared spectroscopy. Both show signatures of accretion and outflow through emission lines of Brackett γ and molecular hydrogen while Haro 6-10N is one of only a few YSOs which display absorption lines from CO and warm organic molecules such as HCN and C_2H_2 (Gibb *et al.* 2008; Doppmann *et al.* 2008). Recently, Roccatagliata *et al.* (2011) have presented high-resolution optical and near-infrared images of Haro 6-10, as well as spectroscopic and interferometric observations in the mid-IR. The results of these observations suggest that Haro 6-10N and Haro 6-10S are embedded in a common envelope, each with a circumstellar disk-like structure. Moreover, the disks are highly misaligned, with the disk around the northern component mostly edge-on and the disk around Haro 6-10S almost face-on.

Multiple outflows are known in the Haro 6-10 region. The dominant outflow is a highly collimated giant Herbig-Haro (HH) flow that extends for 1.6 pc and contains HH 411 and HH 412 (northeast) and HH 410 (southwest) at a position angle of $\sim 222^\circ$ (Devine *et al.* 1999). This outflow was initially associated with Haro 6-10N because of that YSO's more highly obscured, and presumably less evolved, nature. Much closer to Haro 6-10 is the HH 184A-E group which lies about $3'$ (0.12 pc) to the southwest at position angles varying from 225° to 249° . The presence of this lightly obscured HH group led Devine *et al.* to suggest the southwestern flow is blue-shifted. Indeed, a low-velocity bipolar molecular outflow with blue-shifted gas to the southwest and red-shifted gas to the northeast is observed (Stojimirovic, Narayanan, & Snell 2007). A second outflow with a north-south orientation (PA = 175°) is suggested by the one-sided morphology of HH objects 184F-G (Devine *et al.* 1999). A similar orientation relative to Haro 6-10 is seen for a blue-shifted HH jet observed in emission from [S II], [O I], [Fe II], and $\text{Br}\gamma$ with position angles ranging from 175° to 195° (Movsessian & Magakian 1999; Beck, Bary, & McGregor 2010). High resolution radio continuum observations at $\lambda=3.6$ cm have shown a compact radio jet to the southwest of Haro 6-10S at a position angle of 191° that, along with extended $\text{Br}\gamma$ emission, definitively ties the HH jet to the Haro 6-10S (Reipurth *et al.* 2004; Beck *et al.* 2010). Reipurth *et al.* propose that that precession of the outflow, possibly due to a close companion, has shifted the position angle from that of the giant HH flow to that of the Herbig-Haro/radio jet.

Water masers are highly variable tracers of energetic outflows from young stars. Shocks produced as the outflows sweep up ambient material enhance the water abundance and, more importantly, collisionally pump the water molecules to an excited state from which they produce stimulated emission. While the first masers found were associated with young massive stars, water masers are also common around lower mass young stellar objects (YSOs), albeit with a lower duty cycle. Hence it is necessary to monitor lower mass YSOs to detect episodes of maser emission. Single dish monitoring of intermediate-to-low mass YSOs has been used to trigger interferometric observations that track proper motions of water masers and trace their energetic winds (e.g., Claussen *et al.* 1998; Patel *et al.* 2000; Furuya *et al.*

TABLE 1
SUMMARY OF OBSERVATIONS

Telescope ^a	Epoch	Date (YYMMDD)
GBT		031022
GBT		031025
GBT		031109
GBT		031114
GBT		031229
VLBA	I	040106
VLBA	II	040123
GBT		040129
GBT		040202
VLBA	III	040208
VLBA	IV	040223
GBT		040303
VLBA	V	040308
VLBA	VI	040324
GBT		040326
GBT		040409

^aObservations were conducted under proposals AGBT02A_063 (GBT) and BC128 (VLBA).

2005; Imai *et al.* 2007; Marvel *et al.* 2008). Such multi-epoch observations, when separated by periods of weeks, can track individual masers from which one can derive their proper motions, space velocities, as well as the orientation of the wind. Moreover, the lack of extinction by dust at radio wavelengths allows one to observe the maser emission within tens of AUs of the wind origin.

We describe the first detection of water masers from the Haro 6-10 system in 2003 as first reported by Wooten *et al.* (2005). Using both single dish and interferometric radio observations, we first detected and then monitored maser activity associated with Haro 6-10S. Absolute proper motions measured for three masers allowed us to characterize the outflow in terms of the proper motions, space velocities, and position angles of the masers on the sky. In Sec. 2 we describe the observations and the data reduction. The locations and space velocities of the masers are described in Sec. 3. Their relationship to the young binary system and their link to the larger scale molecular outflow and giant HH flow are discussed in Sec. 4.

2. OBSERVATIONS AND DATA REDUCTION

Observations were made using the Green Bank Telescope (GBT) and the Very Long Baseline Array (VLBA), both operated by the National Radio Astronomy Observatory (NRAO) ¹. The single-dish and interferometric radio observations are described below. The telescopes and dates of observations are summarized in Table 1.

2.1. Green Bank Telescope

Haro 6-10 was observed in 2003 October - 2004 April as part of a regular GBT monitoring program of water masers associated with YSOs. Emission from the $6_{16} \rightarrow 5_{23}$ water maser transition at 22.235081 GHz was observed on dates given in Table 1. The 18-22 GHz K-band receiver was used, which has two beams at a fixed separation of $3'$ in azimuth and a beamwidth of about

¹ The National Radio Astronomy Observatory is a facility of the National Science Foundation operated under cooperative agreement by Associated Universities, Inc.

36". The spectrometer was configured to provide channel spacing corresponding to 0.04 km s^{-1} . Data were reduced using the NRAO's AIPS++ program. Once maser activity was observed with the GBT, time was requested to begin observations with the VLBA.

2.2. Very Long Baseline Array

Stations of the VLBA and a single antenna from the Very Large Array were used on six dates beginning in 2004 January and separated by about 16 days (Table 1). The pointing center was the radio continuum position for Haro 6-10S (VLA 1, Reipurth *et al.* 2004). The data from five epochs were reduced using the Astronomical Image Processing System (AIPS classic, Greisen 2003) distributed and maintained by NRAO. The VLBA data were recorded with a 8 MHz bandwidth centered at a velocity of 11.0 km s^{-1} relative to the local standard of rest (LSR). The correlator mode provided a velocity resolution of 0.21 km s^{-1} per channel. Observations of the phase reference source J0426+2327 with a 8MHz bandpass were conducted during each observing period. Bandpass calibration was achieved through observations of 3C 84. Self-calibration on the strongest maser emission was performed using standard methods to extend the dynamic range of the images. After all calibration solutions were determined and applied, the data were mapped using the AIPS task IMAGR. Spectral cubes were formed with pixel cell sizes of $80 \mu\text{arcseconds}$. The beam size was typically $750 \mu\text{arcsec} \times 290 \mu\text{arcsec}$ with a position angle near 0° and the average rms noise was $\sim 5 \text{ mJy}$. We were unable to use data from all of the stations for our 08 February observations and the resulting beam size is about 35% larger. The absolute amplitude calibration is accurate to about 20%.

To retrieve the absolute positional information, the strongest maser was used as the phase reference to image the weak calibrator J0426+2327. Its position relative to the center of the phase-referenced map was equivalent to the position of the Haro 6-10S radio continuum position relative to the strongest maser component. The images of J0426+2327 from each epoch were used to determine the offsets from the phase center in order to measure the absolute position of the strongest maser. The peak flux density of the J0426+2327 varied from 43 - 92 mJy.

3. RESULTS

Despite its inclusion in previous maser surveys, our detection is the first and only report of maser activity in the Haro 6-10 region (e.g., Felli, Palagi, & Tofani 1992; Terebey, Vogel, & Myers 1992; Xiang & Turner 1995; Claussen *et al.* 1996; Furuya *et al.* 2003; Sunada *et al.* 2007). Maser emission mapped with the VLBA has revealed a close association with Haro 6-10S.

3.1. The Radial Velocity of Haro 6-10S

The ambient cloud core in which the binary system resides has a v_{LSR} of 6.4 km s^{-1} with a weaker, contaminating cloud at 4 km s^{-1} (Stojimirovic, Narayanan, & Snell 2007). Estimates for the radial velocity of Haro 6-10S span a range from -6.2 km s^{-1} to 9.4 km s^{-1} and have led Doppmann *et al.* (2008) to suggest it is a radial velocity variable. Published values for v_{LSR} include $3.1 \pm 3.8 \text{ km s}^{-1}$ in 1999 December, $-6.2 \pm 1.5 \text{ km s}^{-1}$ in 2001 November, and $9.4 \pm 1.7 \text{ km s}^{-1}$ in 2007 January

(White and Hillenbrand 2004; Covey *et al.* 2006; Doppmann *et al.* 2008, respectively). Doppmann *et al.* (2008) used these values to fit a model employing a binary companion with a mass of $0.13 M_\odot$, a period of 38 days and a separation from Haro 6-10S of 0.35 AU.

This proposed companion is discrepant with that proposed by Reipurth *et al.* (2004), who suggested the presence of an unseen companion with a separation of 38 AU based on a high resolution image obtained through maximum entropy deconvolution. The companion model supported by Reipurth (2000) links the formation of Herbig-Haro flows to the breakup and ejection of one component from a non-hierarchical triple system.

Fortunately, a high resolution infrared echelle spectrum of Haro 6-10S was taken in August of 2003 which was only 2.5 months prior to our GBT monitoring and 5 months prior to our first VLBA observation. This observation covered the CO lines from $4202\text{-}4267 \text{ cm}^{-1}$ and $4333\text{-}4397 \text{ cm}^{-1}$ and is described in detail by Gibb *et al.* (2007). Using a synthetic spectrum to match the observed CO lines, a radial velocity of $9.5 \pm 1.4 \text{ km s}^{-1}$ is derived. This value is consistent with previous measurements, except for that of Covey *et al.*, and casts doubt on whether Haro 6-10S is a radial velocity variable. From here on, we will reference the radial velocities of the observed maser emission to 9.5 km s^{-1} .

3.2. GBT

The first reported detection of water masers from Haro 6-10 occurred in 2003 October and multiple maser velocities were observed in its spectrum over the next 6 months. These observations, which are shown in Fig. 1, bracketed the VLBA observations. The flux density of the strongest maser component at 11.3 km s^{-1} varied from 15 Jy in 2003 October to a peak of 170 Jy in 2003 December. By 2004 April, the feature had faded to less than 1 Jy. A second, broader feature at 8 km s^{-1} also persisted throughout the monitoring period. Other velocities appeared briefly at 12 and 13 km s^{-1} but had disappeared by 2003 December.

3.3. VLBA

A summary of the maser positions and radial velocities observed from 2004 January through 2004 March are presented in Table 2. Two-dimensional gaussian fits were performed to the maser components in each map using the AIPS task JMFIT. For the first five epochs, from 4-7 distinct components were observed over a sufficient number of velocity channels to permit a gaussian fit to the line profiles. The maser emission was too weak to map in epoch VI. All of the maser components are within 50 milliarcseconds (mas) or 7 AU of the VLA position of Haro 6-10S. Position offsets from the $\lambda = 3.6 \text{ cm}$ position of VLA 1 are given in Table 1 for the peak velocity channel and are accurate to ± 0.5 pixels or $\pm 0.04 \text{ mas}$. All but one of the maser components appear to be red-shifted relative to Haro 6-10S with radial velocities near 11 km s^{-1} . A distinctive and broad 8.3 km s^{-1} , also seen in the GBT spectra, appears to be slightly blue-shifted and lies 15 mas east from the main group.

Because of the proximity of the Taurus region, apparent maser positions must be corrected for variations due to parallax. Corrections derived for the parallactic modulation relative to the center of the parallactic ellipse are

given in Table 3 for the five epochs of VLBA observations. The largest corrections appear between Epochs I and II. We note that Torres *et al.* (2009) have estimated a peculiar velocity of 10.6 km s^{-1} for Taurus sources based on VLBA observations of four YSOs. However, no adjustment was made for a possible drift of Haro 6-10S and the masers due to this motion which would result in an offset of 32 mas to the southeast relative to the radio continuum source position measured in 2002. Based upon their positions, radial velocities, and velocity widths, we were able to track three of the maser components over at least three epochs. The absolute proper motions and the tangential velocities derived from them are given in Table 4. These proper motions have been corrected for the solar motion using the formulation of Abad & Vieira (2005). Using the solar motion relative to the LSR derived from Hipparcos data by Dehnen & Binney (1998), $(U_0, V_0, W_0) = (10.0, 5.25, 7.17) \text{ km s}^{-1}$, the corrections in RA and decl. are $-10.0 \text{ mas yr}^{-1}$ and $-5.30 \text{ mas yr}^{-1}$, respectively. Corrections for Galactic rotation were on the order of 1 mas yr^{-1} or less and not made. The tangential velocities and their uncertainties were computed from a linear least squares fit to the motion over time. Radial velocities in Table 4 are referenced to that of Haro 6-10S. The locations and position angles of the maser tangential velocities are shown in Fig. 2.

Since there is no evidence for a bipolar maser outflow associated with this source as there is in others (e.g., IRAS 05413-0104, Claussen *et al.* 1998), the outflow traced by the three masers apparently locates one side of a bipolar outflow with a velocity on the order of 10 km s^{-1} . The masers have a projected separation of 2 AU with the position angles of the tangential velocities ranging from 196° to 242° , implying an opening angle of the flow of $\sim 45^\circ$. The separating motion of the masers perpendicular to the outflow axis of about 3.5 km s^{-1} can be most simply explained by the opening angle of the wind. The average position angle of 220° is closely aligned with the position angle of the giant HH flow. Their large tangential velocities relative to the radial velocities (Table 4) suggest the flow lies primarily in the plane of the sky. This geometry also explains the apparent presence of red- and blue-shifted masers in the same outflow lobe which has also been observed in the NGC 1333-SVS 13 outflow (Wootten *et al.* 2002). While uncertainties in the radial and tangential velocities could place all three maser spots on the either the redshifted or blueshifted side, the low inclination angle and wide-angle opening angle of the flow are likely to produce both blueshifted and redshifted gas in the same outflow lobe (e.g., Cabrit & Bertout 1986, 1990; Lee *et al.* 2000). An outflow orientation in the plane of the sky is commonly observed in other low mass YSOs with maser emission and is expected if the maser amplification occurs in velocity coherent planar shocks (Claussen *et al.* 1996). The relationship of the masers to known outflows in the region is discussed below.

4. DISCUSSION

It is clear from our maser observations and those of the HH/radio continuum jet, that all of the reported outflow activity originates from the vicinity of Haro 6-10S. Apart from H_2 emission in the spectrum of Haro 6-10N, there is not as yet evidence for an outflow directly related to

this YSO.

It is also apparent that there are two distinct outflows originating from Haro 6-10S. Both the giant HH flow (HH411/412/410, HH184 A-E) and the water masers align along a position angle of $\sim 225^\circ$ and indicate an episodic outflow nearly in the plane of the sky. Working from furthest out to closest in, HH411/410 have dynamical ages of 6000 years; HH184 E an age of 1000 years; HH184 B-C an age of 750 years; and HH184 A an age of 250 years.² Finally, the water masers have a dynamical age estimated from the space velocities given in Table 4 and the distance from the 3.6 cm continuum radio emission of ~ 1 year. The opening angle of 45° for the maser outflow is consistent with the collimation of the outflow increasing as the dynamical age decreases (Arce *et al.* 2007). The episodic nature of HH flows has been discussed by Reipurth (2000) in terms of interactions between components of binary or triple systems and their associated disks. Alternatively, magnetorotational instabilities can lead to rapid accretion events without invoking a close companion (Zhu *et al.* 2009). It is worth noting that the maser space velocities we measure are somewhat lower than those of water masers near driving sources ($20 - 40 \text{ km s}^{-1}$ e.g., Claussen *et al.* 1998; Moscadelli *et al.* 2006; Hirota *et al.* 2008; Marvel *et al.* 2008) of low-mass YSOs and lower than observed from larger scale HH proper motions. It is not unexpected that space velocities of other manifestations of the outflow (e.g., HH objects) are faster than the water masers, since, for both wind-driven and jet bow-shock models, the velocities rise with increasing distance from the source (Arce *et al.* 2007 and references therein).

A second outflow is suggested by the highly blue-shifted (150 km s^{-1}) $\text{Br}\gamma$ emission observed from Haro 6-10S by Beck *et al.* Such radial velocities are consistent an outflow highly inclined to the plane of the sky and with a face-on disk geometry as proposed for Haro 6-10S by Roccatagliata *et al.* (2011). We propose this second outflow is delineated by the radio continuum jet, the compact $\text{Br}\gamma$ and forbidden line emission, and the HH objects HH184 F and G. The position angles measured for these observations all lie in the range of $175^\circ - 195^\circ$. It is important to note that the extended $\text{Br}\gamma$ emission initially has a position angle of $\sim 180^\circ$ before turning toward the southwest at a position angle of $\sim 200^\circ$ (Beck, Bary, & MacGregor 2010).

Having two outflows arising from very close to Haro 6-10S strongly suggests that the driving source is not a single star, but has at least one close-in companion. We estimate that the companion must be at least within 150 mas (20 AU) of Haro 6-10S; otherwise, given the resolution of radio continuum observations ($290 \text{ mas} \times 260 \text{ mas}$, Reipurth *et al.* 2004), a separate source might have been detected depending on its brightness. Indeed, the convergent points for masers A and C and masers B and C lie within 35 mas of the radio continuum position. We speculate that the driving source for the giant HH/maser flow originates from the close-in companion which, due to an edge-on disk, contributes little to the infrared flux from Haro 6-10S. The visible T Tauri star with a face-on disk may be responsible for the highly blue-shifted $\text{Br}\gamma$

² A velocity of $\sim 150 \text{ km s}^{-1}$ was assumed, e.g., Schwartz, Jones & Sirk 1984.

emission. High sensitivity, higher angular resolution observations should be attempted to resolve the putative two stars (this would likely require high frequency radio observations). Our suggestion of a binary nature for Haro 6-10S is unrelated to that suggested by Reipurth et al. (2004), since that binary companion is invoked to drive an apparent east-west radio jet. It is also unlikely to be related to the companion proposed by Doppmann et al. (2008), since the period and separation their proposed companion are much smaller than we require.

5. SUMMARY

We report an outburst of water maser activity from the young binary system Haro 6-10. Using the VLBA over 5 epochs, we were able to track three masers and derive their absolute positions and proper motions. The masers represent one side of a bipolar outflow that lies nearly in the plane of the sky and are clearly associated with the southern component of the binary, the T Tauri star Haro 6-10S. We describe the maser activity as the most recent manifestation of a time-varying bipolar

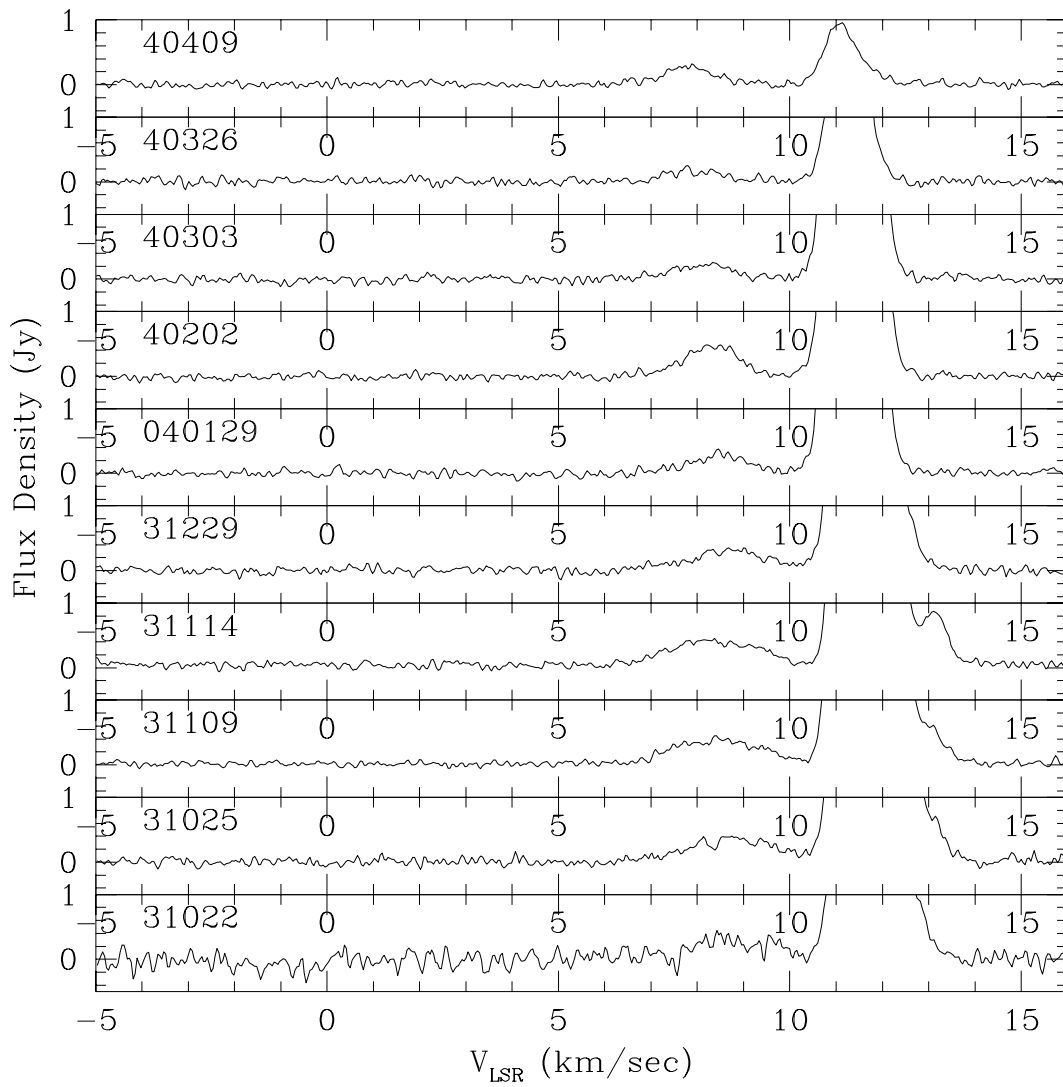
outflow that also includes the giant HH flow: HH 410, HH 411, HH 412, and HH 184A-E. We attribute a jet seen in Br γ , forbidden line, and radio continuum emission and HH 184F-G to a second outflow also clearly associated with the T Tauri star Haro 6-10S. We propose that Haro 6-10S is itself a binary system with a projected separation of <150 mas and speculate that the maser activity originates from the component which is fainter in the infrared. Despite the presence of H $_2$ emission in the spectrum of Haro 6-10N, we do not identify any of the outflows/jets directly to this YSO.

We thank Kari Wojtkowski, Sean Brittain, and Matthew Troutman for assistance with the analysis of the infrared echelle spectra of Haro 6-10. We also thank Prof. Tetsuo Sasao for sharing his code that estimates contributions to the proper motions from the solar motion and galactic rotation. Bradley Gerling gratefully acknowledges a summer internship through the NASA/Missouri Space Grant Consortium.

REFERENCES

- Abad, C. & Vieira, K. 2005, *A&A*, 442, 745
 Arce, H. G., Shepherd, D., Gueth, F. et al. 2007, in *Protostars and Planets V*, ed. B. Reipurth, D. Jewitt, and K. Keil (Tucson, AZ: Univ. Arizona Press), 245
 Beck, T. L., Bary, J. S., & McGregor, P. J. 2010, *ApJ*, 722, 1360
 Cabrit, S. & Bertout, C. 1986, *ApJ*, 307, 313
 Cabrit, S. & Bertout, C. 1990, *ApJ*, 348, 530
 Claussen, M. J., Wilking, B. A., Benson, P. J., Wootten, A., Myers, P. C., & Terebey, S. 1996, *ApJS*, 106, 111
 Claussen, M. J., Marvel, K. B., Wootten, A., & Wilking, B. A. 1998, *ApJ*, 507, L79
 Covey, K. R., Greene, T. P., Doppmann, G. W., & Lada, C. J. 2006, *AJ*, 131, 512
 Dehnen, W. & Binney, J. J. 1998, *MNRAS*, 298, 387
 Devine, D., Reipurth, B., Bally, J., & Balonek, T. J. 1999, *AJ*, 117, 2931
 Doppmann, G. W., Najita, J. R., & Carr, J. S. 2008, *ApJ*, 685, 298
 Elias, J. H. 1978, *ApJ*, 224, 857
 Felli, M., Palagi, F., & Tofani, G. 1992, *A&A*, 255, 293
 Furuya, R., Kitamura, Y., Wootten, A., Claussen, M. J., & Kawabe, R. 2003, *ApJS*, 144, 71
 Furuya, R. S., Kitamura, Y., Wootten, A., Claussen, M. J., & Kawabe, R. 2005, *A&A*, 438, 571
 Gibb, E. L., Van Brunt, K. A., Brittain, S. D., & Rettig 2007, *ApJ*, 660, 1572
 Gibb, E. L., Van Brunt, K. A., Brittain, S. D., & Rettig 2008, *ApJ*, 686, 748
 Goodrich, R. W. 1986, *AJ*, 92, 885
 Greisen, E. W. 2003, in "Information Handling in Astronomy — Historical Vistas", ed. A. Hech (Dordrecht: Kluwer Academic Publishers), 109
 Hirota, T. et al. 2008, *PASJ*, 60, 37
 Imai, H. et al. 2007, *PASJ*, 59, 1107
 Lee, C.-F., Mundy, L. G., Reipurth, B., Ostriker, E. C., & Stone, J. M. 2000, *ApJ*, 542, 925
 Leinert, Ch. & Haas, M. 1989, *ApJ*, 342, L39-L42
 Marvel, K. B., Wilking, B. A., Claussen, M. J, & Wootten, A. 2008, *ApJ*, 685, 285
 Menard, F., Monin, J.-L., Angelucci, F., & Rouan, D. 1993, *ApJ*, 414, L117
 Moscadelli, L., Testi, L., Furuya, R. S., Goddi, C., Claussen, M., Kitamura, Y., & Wootten, A. 2006 *A&A*, 446, 985
 Movsessian, T. A. & Magakian, T. Y. 1999, *A&A*, 347, 266
 Patel, N. A., Greenhill, L. J., Herrnstein, J., Zhang, Q., Moran, J. M. et al. , *ApJ*, 538, 268
 Reipurth, B. 2000, *AJ*, 1290, 3177
 Reipurth, B., Rodriguez, L. F., Anglada, G., & Bally, J. 2004, *AJ*, 127, 1736
 Roccatagliata, V., Ratzka, Henning, T., Wolf, S., Leinert, C., & Bouwman, J. 2011, *A&A*, 534, 33
 Stojimirovic, I., Narayanan, G., & Snell, R. L. 2007, *ApJ*, 660, 418
 Schwartz, R., Jones, B. F., & Sirk, M. 1984, *AJ*, 89, 1735
 Sunada, K., Nakazato, T., Ikeda, N., Hongo, S., Kitamura, Y., & Yang, J. 2007, *PASJ*, 59, 1185
 Terebey, S., Vogel, S. N., & Myers, P. C. 1992, *ApJ*, 390, 181
 Torres, R. M., Loinard, L., Mioduszewski, A. J., & Rodriguez, L. F. 2009, *ApJ*, 698, 242
 White, R. J., & Hillenbrand, L. A. 2004, *ApJ*, 616, 998
 Wootten, A., Claussen, M., Marvel, K., & Wilking, B. 2002, in *IAU Symposium 206, Cosmic Masers: From Proto-Stars to Black Holes*, eds. V. Mineese & M. Reid (San Francisco: Astronomical Society of the Pacific), 100
 Wootten, A., Claussen, M., Marvel, K., & Wilking, B. 2005, in *Protostars and Planets V, Proceedings of the Conference held October 24-28, 2005, LPI Contribution No. 1286*, 8595
 Xiang, D. & Turner, B. 1995, *ApJS*, 99, 121
 Zhu, Z., Hartmann, L., Gammie, G., & McKinney, J. C. 2009, *ApJ*, 701, 620

Figure Captions



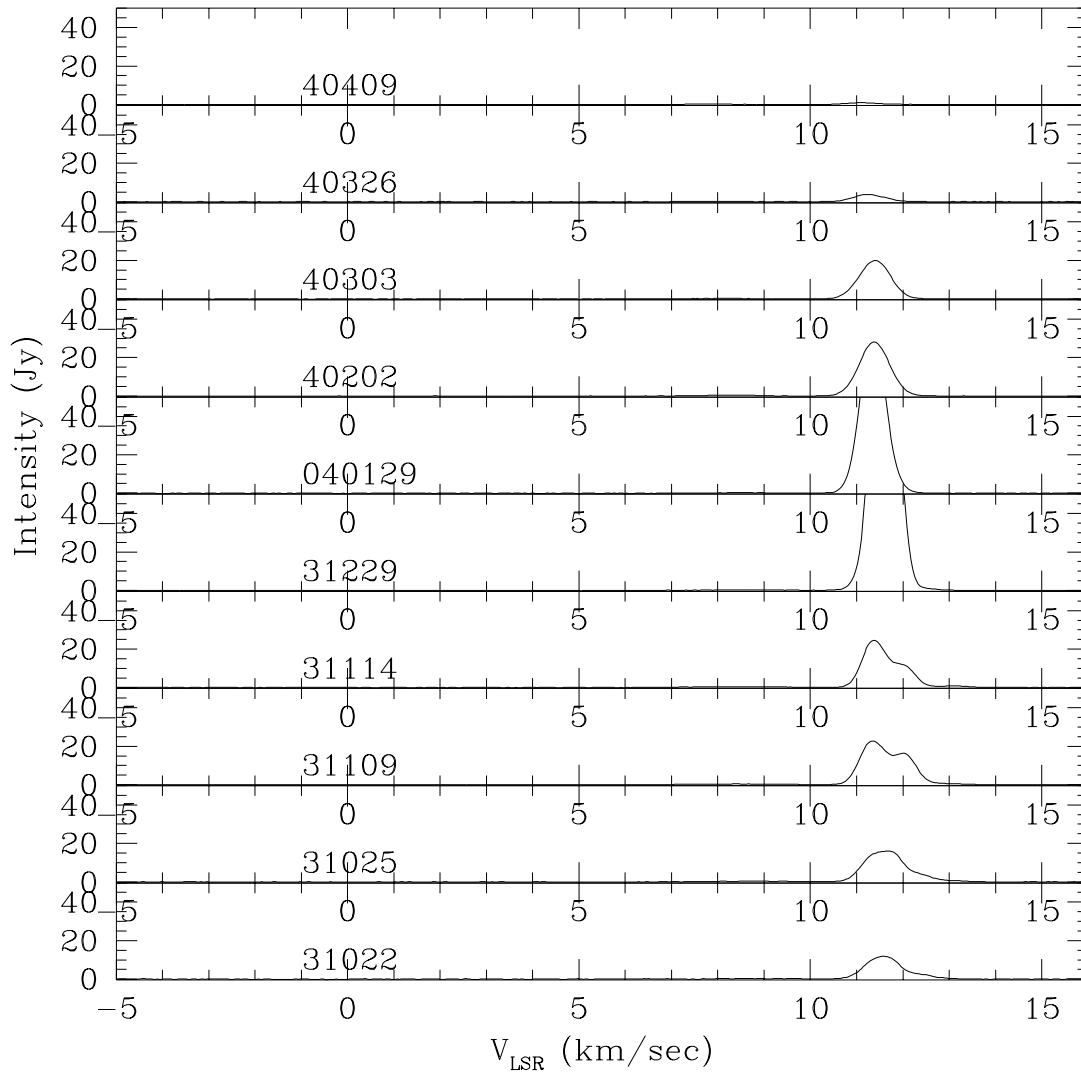


FIG. 1.— GBT spectra of the Haro 6-10 masers. Fig. 1a shows emission less than 1 Jy, focusing on the weaker emission components. Fig. 1b shows emission less than 50 Jy and emphasizes the strongest maser emission.

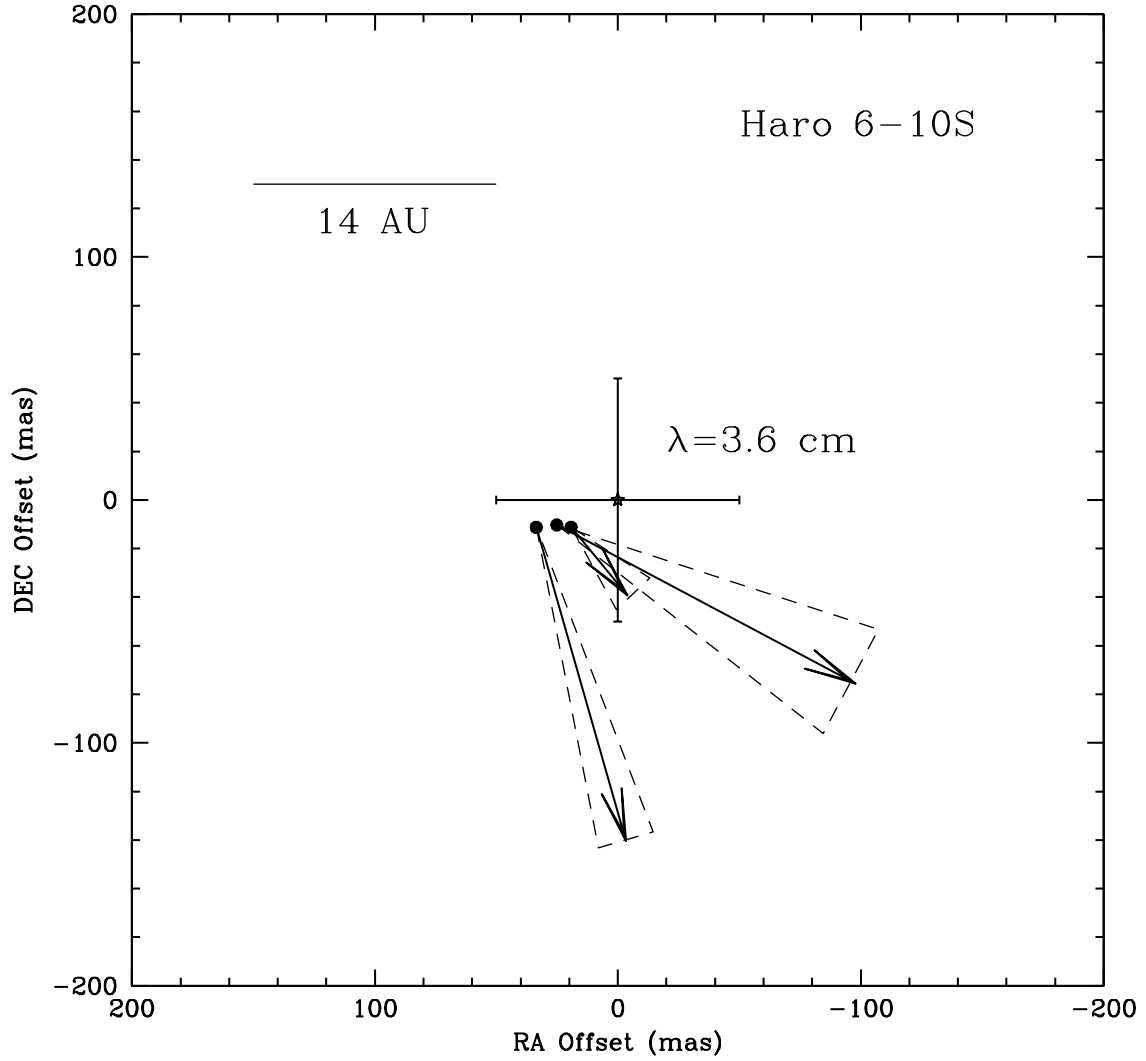


FIG. 2.— Absolute motions for three maser components. The (0,0) position is the radio continuum position of Haro 6-10S (R.A.(2000) $4^h 29^m 23.733^s$, decl.(2000.0) $+24^\circ 33' 00.12''$, Reipurth *et al.* 2004). Solid arrows mark the proper motion vectors, projected over a ten year period for display purposes. Errors on the proper motion magnitudes are given in Table 4. The dashed lines delineate the uncertainties in the position angles.

TABLE 2
FITTED GAUSSIAN COMPONENTS

Epoch ID	Other	Julian Date	X offset ^a (mas)	Y offset (mas)	Radial Velocity (km s ⁻¹)	Peak Flux (Jy)	FWHM (km s ⁻¹)
I-A		2453010.70	15.04	-11.54	11.3	35	0.69
I-B			14.16	-12.01	11.2	6.2	0.60
I-C			22.93	-10.83	12.1	0.44	0.50
I-D			13.36	-11.46	11.3	0.69	0.65
I-E			12.16	-11.42	11.1	0.44	0.48
II-A	I-A	2453027.65	13.38	-12.58	11.1	25	0.65
II-B			19.47	-10.97	11.0	0.52	0.49
II-C			27.90	-11.95	8.3	0.32	0.95
II-D			13.76	-12.32	11.2	8.5	0.86
II-E			12.96	-12.84	11.1	4.3	0.80
III-A	II-A	2453043.61	12.44	-13.28	11.1	35	0.62
III-B	II-B		17.69	-11.97	10.8	1.7	0.55
III-C	II-C		27.16	-13.08	8.5	0.10	0.85
III-D			11.89	-12.61	11.2	2.6	0.60
IV-A	III-A	2453059.56	12.21	-14.08	11.2	4.0	0.50
IV-B	III-B		17.27	-12.85	11.0	0.81	0.40
IV-C	III-C		27.11	-14.41	8.2	0.18	0.70
IV-D			11.54	-13.23	11.2	1.8	0.55
IV-E			12.62	-13.79	11.1	6.1	0.82
IV-F			17.54	-12.66	10.9	0.80	0.58
V-A		2453073.50	12.53	-14.46	11.5	5.1	0.59
V-B			11.86	-13.73	11.3	2.2	0.55
V-C			11.49	-13.48	11.1	2.0	0.70
V-D			19.94	-11.41	11.0	0.46	0.40
V-E			18.34	-13.09	10.9	0.25:	0.55:
V-F			17.71	-13.12	10.9	0.66	0.69
V-G			12.67	-14.38	11.0	0.91	0.76

^aOffsets are positive east and north from the $\lambda = 3.6$ cm radio continuum source VLA 1 (RA(2000) = $4^{\text{h}}29^{\text{m}}23.733^{\text{s}}$, DEC(2000) = $+24^{\circ}33'00.12''$). Offsets in Epoch V are uncertain due to a possible 2-3 pixel shift in the reference maser position.

TABLE 3
CORRECTIONS FOR PARALLACTIC MODULATION

Epoch ID	Julian Date	μ_{α}^{a} (mas yr ⁻¹)	μ_{δ}^{a} (mas yr ⁻¹)
I	2453010.75	-4.218	-0.379
II	2453027.75	-5.711	-0.683
III	2453043.75	-6.642	-0.913
IV	2453059.75	-7.043	-1.069
V	2453073.75	-6.940	-1.137

^aCorrections are to be subtracted from the values in Table 2.

TABLE 4
MASER PROPER MOTIONS AND VELOCITIES

Parameter	Maser I-A - IV-A	Maser II-B - IV-B	Maser II-C - IV-C
μ_α (mas yr ⁻¹)	-0.10±1.17	-9.86±5.54	6.17±1.07
μ_δ (mas yr ⁻¹)	-13.54±0.67	-17.10±0.35	-23.65±1.83
$\mu_{\alpha,corr}^a$ (mas yr ⁻¹)	-2.62	-12.38	-3.65
$\mu_{\delta,corr}^a$ (mas yr ⁻¹)	-2.83	-6.39	-12.94
μ_{total} (mas yr ⁻¹)	3.86	13.93	13.44
V_{tan} (km s ⁻¹)	2.6±0.6	9.3±3.3	9.0±1.2
PA ^b (degrees)	223±14	242±10	196±5
V_{rad}^c (km s ⁻¹)	1.6	1.4	-1.2
V_{space} (km s ⁻¹)	3.0	9.4	9.1

^aProper motion correction for the solar motion.

^bPosition angle in the plane of the sky measured east of north declination.

^cRadial velocity relative to that measured for Haro 6-10S in August 2003.